Wave packets falling under a mirror

2002 J. Phys. A: Math. Gen. 35 9829

(http://iopscience.iop.org/0305-4470/35/46/308)

INSTITUTE OF PHYSICS PUBLISHING JOURNAL OF PHYSICS A: MATHEMATICAL AND GENERAL

J. Phys. A: Math. Gen. **35** (2002) 9829–9841 PII: S0305-4470(02)39155-8

Wave packets falling under a mirror

G Kälbermann

Soil and Water Department, Faculty of Agriculture, Rehovot 76100, Israel

E-mail: hope@vms.huji.ac.il

Received 5 July 2002, in final form 9 October 2002
Published 7 November 2002
Online at stacks.iop.org/JPhysA/35/9829

Abstract

We depict and analyse a new effect for wave packets falling freely under a barrier or well. The effect appears for wave packets whose initial spread is smaller than the combination $\sqrt{l_g^3/|z_0|}$, between the gravitational length scale $l_g = (\hbar^2 c^2/2m^2 g)^{1/3}$ and the initial location of the packet z_0. It consists of a diffractive structure that is generated by the falling and spreading wave packet and the waves reflected from the obstacle. The effect is enhanced when the Gross–Pitaevskii interaction for positive scattering length is included. The theoretical analysis reproduces the essential features of the effect. Experiments emanating from the findings are proposed.

PACS numbers: 03.65.Nk, 42.25.Fx, 03.75.Fi

1. Introduction

In the past years we have described a new phenomenon called: *wave packet diffraction in space and time* [1–5]. The phenomenon occurs in wave packet potential scattering for the nonrelativistic Schrödinger equation and for the relativistic Dirac equation. The effect consists in the production of a multiple-peak structure that travels in space and persists. This pattern was interpreted in terms of the interference between the incoming spreading wave packet and the scattered wave. The patterns are produced by a time-independent potential in the backward direction, in one dimension, and, at large angles, in three dimensions. The multiple-peak wave train exists for all packets, but it does not decay only for packets that are initially thinner than $\sqrt{\frac{w}{q}}$, where w is a typical potential range or well width and q is the incoming average packet momentum. For packets that do not obey this condition the peak structure eventually merges into a single peak. The effect appears also in forward and backward scattering of wave packets from slits [5].

The experimental breakthrough of Bose–Einstein condensation in clusters of alkali atoms [6, 7][1] leads to the reinvestigation of the influence of the earth's gravitational field on the development of a quantum system.

Gravity is currently being advocated as a means of allowing the extraction of atoms from the condensate for the realization of an atom laser continuous output coupler [8–10]. Despite the weakness of the gravitational force on earth, it has a major influence on atoms that are cooled to micro-Kelvin temperatures. It is then necessary to include the effects of gravity in theoretical calculations with condensates.

Many other gravitational effects with quantum systems are being considered nowadays, such as bound states of neutrons in a gravitational field above a mirror, [11], or the use of the coherence properties of condensates to serve as interferometers in the presence of gravity [12, 13].

The Bose–Einstein condensate in a magnetic trap is in reality a wave packet. To the extent that decoherence effects are not dominant, it is expected to evolve in a gravitational field in the same manner as a Schrödinger wave packet. In the present work we investigate the effects of gravity on falling packets.

It will be shown numerically and analytically that packets falling *under* an obstacle but, free from below, display distinctive quantum features due to their wave nature.

The Schrödinger wave packets not only fall, but also spread. The thinner the initial extent of the packet the broader the spectrum of momenta it carries. Consequently, it will generate many more components able to reflect from the obstacle, be it a well or a barrier. These reflected waves will interact with the spreading and falling packet.

There exists a crossover length scale, at which the interfering pieces start to produce a diffractive coherent structure that travels in time, analogous to the effect of wave packet diffraction in space and time previously investigated [1–5].

This length scale is $\sqrt{\frac{l_g^3}{|z_0|}}$, with $l_g = \left(\frac{\hbar^2 c^2}{2m^2 g}\right)^{1/3}$. For sodium atoms l_g is about 0.73 μm while for hydrogen it is 5.86 μm.[2] For packets *initially* narrower than a proportion of this scale, the effect is extremely evident, and gets blurred the wider the initial packet. This effect may be observed with the same setup as the one used in Bose–Einstein condensation experiments, provided pencil-like, thin packets are produced and allowed to fall under a roof [12].

We will provide analytical approximations to the exact solution of the problem that reproduce quite satisfactorily the numerical results. In section 2 we present numerical results. Section 3 will deal with theoretical aspects. Section 4 summarizes the paper and provides concluding remarks regarding possible experiments.

2. Packets falling under a roof

Matter wave diffraction phenomena in time [14, 15] induced by the sudden opening of a slit, or in space by fixed slits or gratings, are understood simply by resorting to plane wave monochromatic waves.

Atomic wave diffraction experiments [16], have confirmed the predictions of diffraction in time [14] calculations. These patterns fade out as time progresses.

The phenomenon of diffraction of wave packets in space and time was presented in [1–5]. It consists of a multiple-peak travelling structure generated by the scattering of initially thin

[1] A comprehensive bibliography on Bose–Einstein condensation may be found at the JILA site http://bec01.phy.GaSoU.edu/bec.html/bibliography.html.

[2] In the following, we will use $\hbar = 1$, $c = 1$. The units of length are microns, of time, milliseconds, with $g = 9.8 \frac{\mu\text{m}}{\text{ms}^2}$.

packets from a time-independent potential, a well, a barrier or a grating. The condition for the pattern to persist was found to be

$$\sigma \ll \sqrt{\frac{w}{q_0}} \tag{1}$$

where σ is the initial spread of the packet, w is the width of the well or barrier and q_0 is the impinging packet average momentum. For packets broader than this scale the diffraction pattern mingles into a single broad peak.

The original motivation for the present work was the addition of gravity to the potential affecting the packet propagation. As described above, the effects of gravity become increasingly relevant to the dynamics of packets in traps and elsewhere.

The educational literature abounds in works dealing with the dynamics of packets falling on a mirror. The so-called *quantum bouncer* [17] is a clean example of the use of the Airy packet in the treatment of the problem. The use of the Airy packet is straightforward above the mirror with the boundary condition of a vanishing wavefunction at the location of the mirror, and becomes a nice laboratory for the investigation of the quantum classical correspondence, revivals, the Talbot effect, etc. Falling packets were not studied, perhaps in light of the preconception that nothing interesting will be found besides the expected spread and free fall of the packet.

However, there is a surprise awaiting us here. This is not totally unexpected due to the wave nature of the packet that consists of modes propagating in both the downward and the upward directions. Analogous effects are apparent also when a packet propagates parallel to a mirror without ever getting close to it [18]. Again the spreading and interference between the incoming and reflected waves produce a wealth of phenomena.

In this section, we present the numerical results for the falling of packets under a barrier or well using Gaussian wave packets. The use of Gaussian packets permits a straightforward connection to theoretical predictions.

The scattering event starts at $t = 0$ with a minimal uncertainty wave packet

$$\Psi_0 = A\,\mathrm{e}^{\mathrm{i}\alpha} \qquad \alpha = q(z - z_0) - \frac{(z - z_0)^2}{4\sigma^2} \tag{2}$$

centred at a location z_0 large enough for the packet to be almost entirely outside the range of the potential. σ denotes the width parameter of the packet. $q = mv$ is the average momentum of the packet. The potential affecting the packet is a square well, the gravitational interaction and eventually the Gross–Pitaevskii (GP) interaction, that subsumes the effects of forces between the atoms in the condensate in the mean field approximation [19]

$$V = mgz + U\Theta(w/2 - |z - w/2|) + \alpha|\Psi|^2 \tag{3}$$

where m is the mass of the atom taken here to be sodium, w is the width of the well or barrier, of depth or height U and α is the strength of the GP interaction [19], which using the scattering length of sodium and a typical number of atoms in a trap of the order of 250 atoms $\mu\mathrm{m}^{-3}$ yields $\alpha \approx 25$ for a wavefunction normalized to one.

Figure 1 depicts the setup of the problem. A thin wave packet is initially located around a point $z_0 = -7\,\mu$m under a thick barrier, the mirror. The mirror could be any flat surface. We have represented the strength of the barrier by means of a square located above $z = 0$. The simplification of the present investigation assumes the mirror to be a finite width plate of thickness $t = 10\,\mu$m in the figure extending to a much larger distance along the x, y plane. For the one-dimensional calculation we took a thin packet along the z *axis* of width $4\sigma \approx 0.4\,\mu$m. It is supposed to be a pencil-like packet whose extension along the x, y plane is larger than the width, such that the quantum dispersion affects primordially the behaviour of the packet

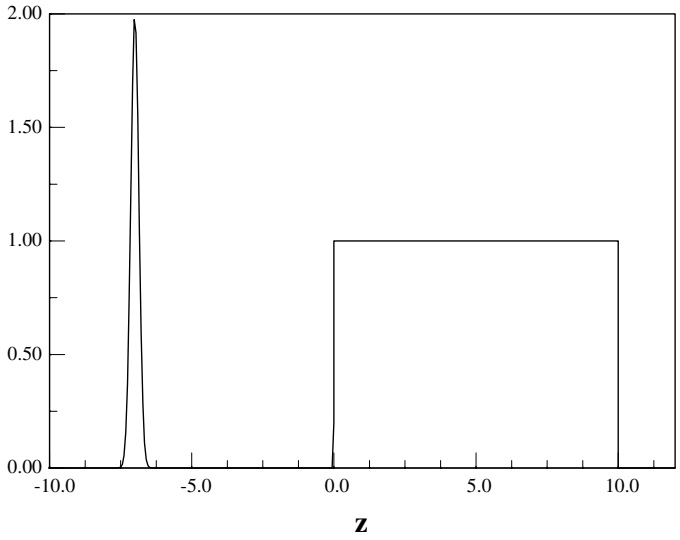

Figure 1. Setup of the problem. The packet's initial location is $z_0 = -7\,\mu$m. The mirror is depicted as a square of arbitrary height representing the strength of the repulsive potential. The mirror is located above $z = 0$ and its width is $10\,\mu$m.

along the vertical direction. In this direction, the packet falls freely. The interference between the packet components reflected from the barrier, upward moving waves, and those that fall freely without reflection, the downward moving ones, will induce a diffraction pattern. We will find that the contrast of the pattern depends crucially on the initial location of the packet and its width.

An ideal implementation of this setup would be to use a Bose–Einstein condensate optically trapped in a region below a plate. Then stop the confining potential and let it fall freely under the plate.

The condition for the observation of the effect would be to produce a thin enough condensate. For repulsive Gross–Pitaevskii interactions as in sodium, rubidium or hydrogen, the width limitation is less stringent, as will be shown below. The extra repulsion of the interaction, on top of the quantum dispersion, effectively pushes the waves inside the condensate against the wall. It acts as if the packet was initially thinner than it actually is. In particular, for hydrogen the initial width of the packet may be as large as a few microns. In section 4, we make some further comments concerning the relevance of the effect for atom lasers.

The algorithm for the numerical integration of the Schrödinger equation of the present work is described in previous works [1–3]. Flux conservation for initially normalized packets and energy conservation require that

$$\begin{aligned} 1 &= \int_{-\infty}^{\infty} |\Psi(z,t)|^2 \,\mathrm{d}z \\ E &= \int_{-\infty}^{\infty} \left[\frac{1}{2m} \frac{\partial \Psi(z,t)}{\partial z} \frac{\partial \Psi^*(z,t)}{\partial z} + \left(mgz + V(z) + \frac{\alpha}{2} |\Psi(z,t)|^2 \right) |\Psi(z,t)|^2 \right] \mathrm{d}z \end{aligned} \tag{4}$$

with E a constant independent of time.

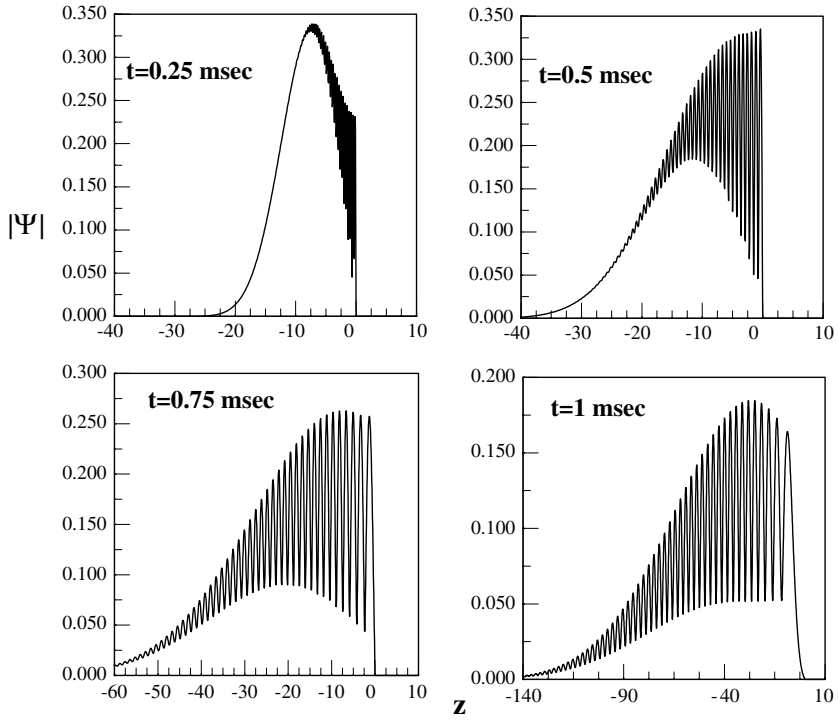

Figure 2. Time evolution of a packet profile of initial location $z_0 = -7\,\mu$m falling under the repulsive barrier (not depicted).

The numerical runs presented below achieved an accuracy in the flux conservation of around 0.2%, while the accuracy in the energy conservation was around 2%. The wavefunction was also found to obey the Schrödinger equation to an accuracy better than the 1% level even at points near the edges of the integration range.

The only length scale appearing in the problem is easily derived from the Schrödinger equation to be l_g. For sodium this is $l_g = 0.73\,\mu$m.

We consider the free fall of packets with initial widths σ smaller and larger than a fraction of l_g with or without the GP interaction. We take the barrier to have the fixed strength of $U = 10^6\,\mathrm{s}^{-1}$ obtained from $U \approx = \frac{4\pi a}{m}N$, with a, the scattering length of the sodium-solid scattering and N the density of a typical solid. For the well we use a value taken from a van der Waals type of strength [20] at a distance of 1 nm, namely $U \approx -10^2\,\mathrm{s}^{-1}$. We used a very high value for the attractive well strength, beyond the limit of applicability of the Lennard-Jones formula [20], to see whether even a large and unrealistic value for the attractive potentials influences the results as compared to the repulsive case.

Figure 2 shows the time evolution of a thin packet falling under a mirror. This is essentially what is expected to be observed in an actual imaging of a Bose–Einstein condensate falling freely under a mirror as a function of time. The figure shows the results for sodium, however, as mentioned above the same will occur with a hydrogen condensate, with much wider packets initially.

Figure 3 shows wide and thin packet profiles after 4 ms fall under a repulsive barrier.

The behaviour of a thin packet is qualitatively different. A wide packet falls undistorted except for the natural spreading. A thin packet whose width is smaller than $\sqrt{\frac{l_g^3}{|z_0|}}$ (see below

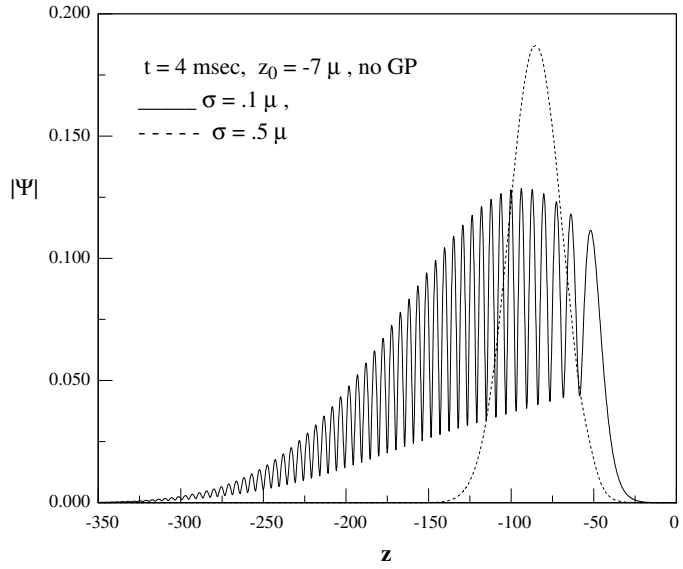

Figure 3. Packet profiles of initial location $z_0 = -7\,\mu$m after $t = 4$ ms falling under a repulsive barrier.

for the appearance of z_0 in the expression), possesses a distinctive diffractive structure. The rightmost (upper) edge of the structure resembles the Airy packet absolute value, however, the packet drops exponentially at large $|z|$ values, whereas the Airy packet diminishes as $|z|^{-1/4}$. In the next section we will address a theoretical approach to the problem. Approximate analytical solutions will be provided that reproduce the basic features of both the thin and wide packets.

In figure 4, we present an analogous picture for the case including the GP interaction. As expected [19], the distinctive feature of the inclusion of this interaction is an extra repulsive force, due to the positive scattering length, that enhances the broadening of the packet, and consequently the diffraction effect. As seen from the figure, for the same values of initial packet widths, the nonlinear repulsive interaction produces a much cleaner interference pattern than the case lacking it in figure 3.

Figure 5 depicts the influence of the GP interaction on the packet profiles for initially thin packets.

The GP force produces a diffractive structure that has a much starker contrast. Large momenta are excited by the repulsive interaction, producing a more effective superposition between incoming and reflected waves.

We argued that the appearance of a diffractive structure is determined by the ratio $\epsilon = \frac{\sigma}{\sqrt{l_g^3/|z_0|}}$. Figure 6 shows the results when this ratio is around 1. While the pattern has almost disappeared from the falling packet devoid of GP interaction, it has lost contrast, but not disappeared completely from the packet subjected to the GP force. ϵ is then the relevant ratio for the appearance of the diffractive structure.

Replacing the barrier by a well has no effect whatsoever for packets without initial momentum. The higher the initial momentum of the packet (if positive), the easier the transmission through the well. The differences arise then for packets thrown against the obstacle only at large momenta as compared to l_g^{-1}. This point will be dealt with in the future.

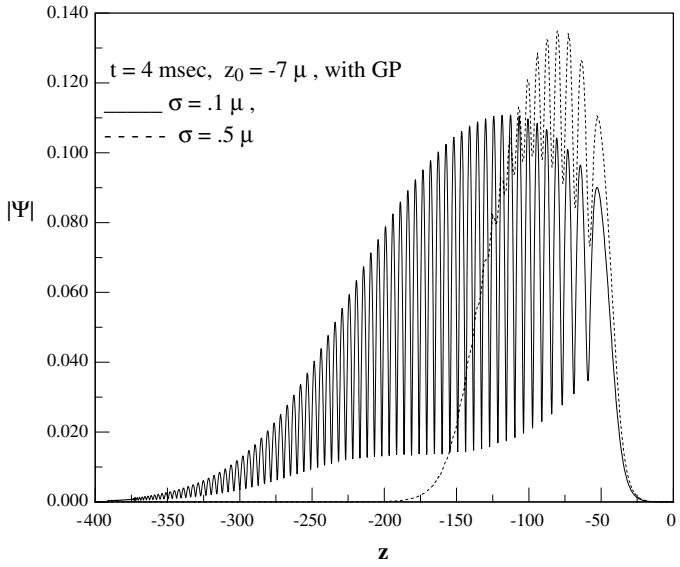

Figure 4. Packet profiles of initial location $z_0 = -7\,\mu$m after $t = 4$ ms falling under a repulsive barrier and subject to the Gross–Pitaevskii interaction.

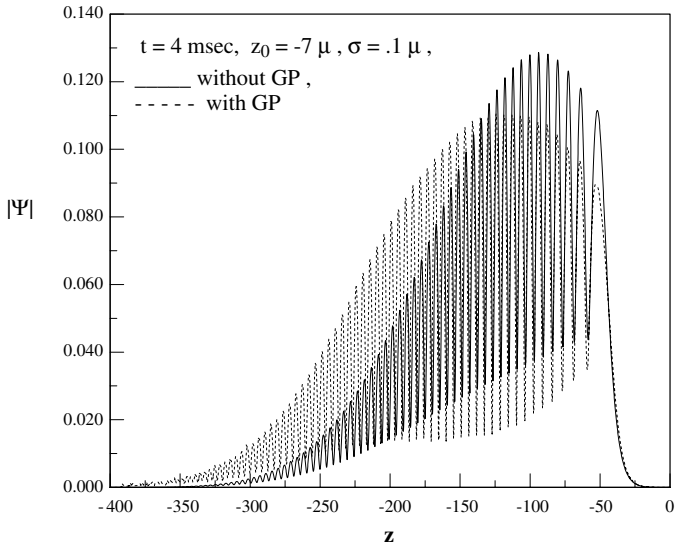

Figure 5. Thin packet profiles after $t = 4$ ms of fall under a repulsive barrier with and without the Gross–Pitaevskii interaction.

3. Theoretical approach to falling packets

The Airy function [21] is the solution of the Schrödinger equation for propagation in a uniform field. Despite being named the Airy packet, it is not normalizable and belongs to the set of wavefunctions in the continuum. It is the analogue of a plane wave in free space.

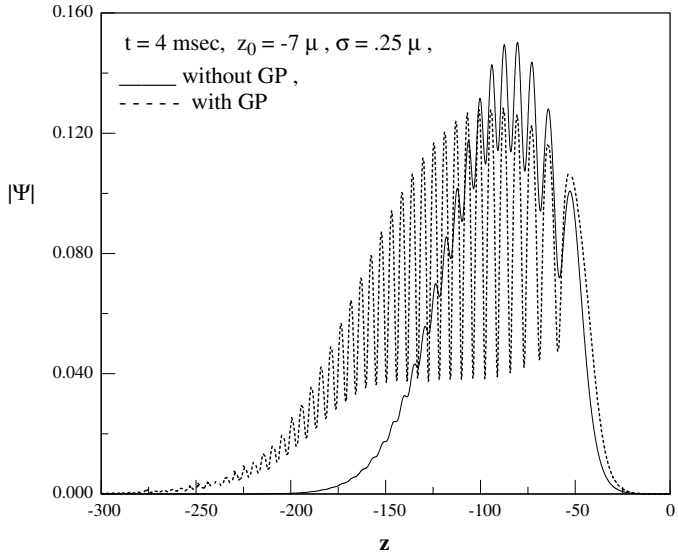

Figure 6. Borderline packet profile after $t = 4$ ms of fall under a repulsive barrier without and including the Gross–Pitaevskii interaction.

The educational literature abounds in references to uses of this packet, both in the context of the *quantum bouncer* [17] and in the treatment of generalized Galilean transformations [22].

For the solution of a packet falling on a mirror, the *quantum bouncer*, the Airy functions shifted to positions that have a zero at $z = 0$, serve as a basis to find the time development of an arbitrary initial packet.

The lower piece of the Airy packet is oscillatory and does not decay fast enough to serve as a basis for packets initially located under the mirror. Only when a continuum of energies (both positive and negative) is used, it is possible to expand an initial wave packet located at $z < 0$ in terms of Airy functions.

Before analysing the problem by means of Airy functions, we will develop a very simple approximation that allows the identification of the relevant length scale for the effect to occur.

We will resort to a set of solutions that connects directly to plane waves. These solutions are not stationary in the rigorous sense of the word, because they have a time-dependent phase that is not linear in time. The solutions are derived by transforming a plane wave to an accelerating frame [22–25], namely

$$\chi_k(z,t) = \mathrm{e}^{\mathrm{i}\phi} \qquad \phi = -mgzt + k\left(z + \frac{gt^2}{2}\right) - \frac{k^2}{2m}t - \frac{mg^2t^3}{6}. \tag{5}$$

Direct substitution in the Schrödinger equation proves that this family of solutions solves the equation for a potential $V = mgz$.

Given that the initial wave packet of equation (2) may be expanded readily in plane waves that coincide with equation (5) at $t = 0$, the Schrödinger equation then ensures that the subsequent propagation of the packet will be obtained by replacing the plane waves by the solutions in the gravitational potential of equation (5).

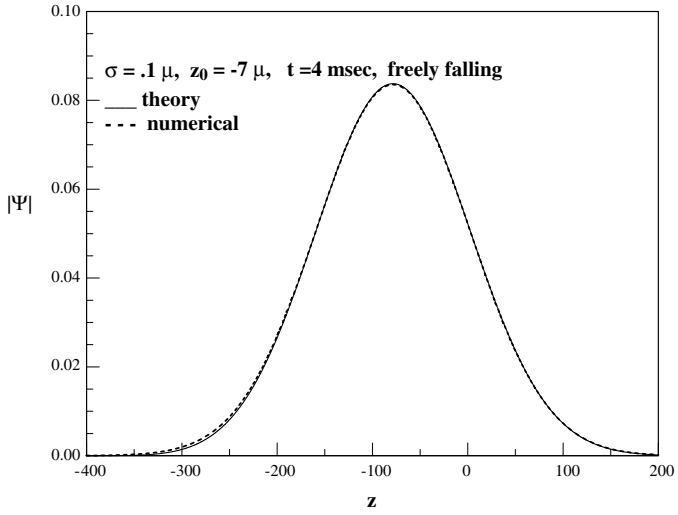

Figure 7. Profile of a packet of initial width $\sigma = 0.35\ \mu$m and initial location $z_0 = -7\ \mu$m in free fall after $t = 4$ ms. Numerical calculation (dotted line) and theoretical formula of equation (6) (full line).

We find the expression at all times for a freely falling normalized Gaussian packet

$$\Psi(z - z_0, t) = \frac{e^{\xi}\chi_q(z - z_0, t)\sqrt{\sigma}}{\sqrt{\sqrt{2\pi}\sigma^2(t)}}$$
$$\xi = \frac{(z - z_0 + gt^2/2 - q/mt)^2}{4\sigma^2(t)} \tag{6}$$
$$\sigma^2(t) = \frac{it}{2m} + \sigma^2.$$

Figure 7 depicts the comparison between the expression of equation (6) and a numerical calculation. The agreement is satisfactory without any rescaling. It lends confidence in both the numerical scheme and the theoretical formulae.

At $t = 0$ we can readily build a packet that solves the problem with the boundary condition of $\Phi(0) = 0$, corresponding to an impenetrable mirror at $z = 0$. Just an image packet located at $-z_0$ in the inaccessible region above the mirror will serve. The solution at $t = 0$ then becomes $\Phi(z, t = 0) = \Psi(z - z_0, 0) - \Psi(z + z_0, 0)$, with Ψ in equation (6). Φ obeys the equation of motion and the boundary condition. It also coincides with the initial packet of equation (2) in the allowed region of $z < 0$. Propagating Φ forward in time we obtain

$$\Phi(z, t) \approx \Psi(z - z_0, t) - \Psi(z + z_0, t). \tag{7}$$

We write the approximate sign, because the cancellation at $z = 0$ is only effective at short times. As soon as t increases, the wavefunction of equation (7) does not vanish any more. Presumably, an infinite set of image packets is needed.

We could not find a closed analytical solution at all times. The solution of equation (7) reproduces reasonably well the falling packets and distinguishes clearly between a packet narrower than l_g and one wider than l_g for z_0 of the order of a few packet widths. In order to

see this we write the absolute value of equation (7) for a packet with initial momentum $q = 0$ for $t \gg 2m\sigma^2$

$$
\begin{aligned}
|\Psi(z,t)| &= A\,\mathrm{e}^{\theta_1}\sqrt{\sin^2(\theta_2)+\sinh^2(\theta_3)}\\
\theta_1 &= -\frac{m^2\sigma^2\left((z+gt^2/2)^2+z_0^2\right)}{4t^2}\\
\theta_2 &= \frac{mz_0(z+gt^2/2)}{t}\\
\theta_3 &= \frac{m^2\sigma^2 z_0(z+gt^2/2)}{2t^2}.
\end{aligned}
\tag{8}
$$

θ_3 is responsible for the blurring and loss of contrast of the diffraction pattern determined by the sine function. The larger θ_3 is the less visible are the oscillations. The criterion for the visibility of the pattern may then be written as $\max(\theta_3) \ll 1$. The maximum value of $-z$ is given by the descent of the packet and its spreading. Both are of the order of $\frac{gt^2}{2}$. We can then write the condition for the visibility of the interference fringes to be

$$
\max(\theta_3) \approx \frac{m^2\sigma^2|z_0|g}{2} \ll 1. \tag{9}
$$

Hence we can write equation (9) as

$$
\sigma \ll 2\sqrt{\frac{l_g^3}{|z_0|}}. \tag{10}
$$

Equation (10) demonstrates that the relevant borderline between a visible and a blurred packet is $\sigma = \sqrt{\frac{l_g^3}{|z_0|}}$. A packet initially narrower than l_g located at a distance a few times its width under a mirror will definitely display interference fringes. Equation (8) also tells us that this pattern travels with the packet unscathed.

We now proceed to find a solution in terms of Airy functions[3].

A solution of the mirror problem for $z < 0$ can be determined by means of a set of functions that solve the freely falling packet, namely linear combinations of the independent Airy functions Ai *and* Bi [26]. A set that implements the boundary condition of a vanishing wavefunction at the origin reads

$$
\chi_a(x) = (\mathrm{Bi}\,(a)\,\mathrm{Ai}\,(x+a) - \mathrm{Ai}\,(a)\,\mathrm{Bi}\,(x+a))/\sqrt{\mathrm{Ai}^2(a)+\mathrm{Bi}^2(a)} \tag{11}
$$

where $x = \frac{z}{l_g}$, $a = \frac{-E}{mgl_g}$, with E, the energy of a stationary solution $-\infty < a < \infty$.

The functions obey

$$
\int_{-\infty}^{0} \chi_a(x)\chi_b(x)\,\mathrm{d}x = \delta(a-b) \tag{12}
$$

with δ, the Dirac δ function. The set is orthonormal and complete.

The initial wave packet of equation (2) is expanded in terms of the above set as

$$
\begin{aligned}
\Psi(x,t=0) &= \int_{-\infty}^{\infty} C(a)\chi_a(x)\,\mathrm{d}a\\
C(a) &= \int_{-\infty}^{0} \chi_a(x)\Psi(x,t=0)\,\mathrm{d}x.
\end{aligned}
\tag{13}
$$

[3] The author wishes to express his gratitude for the extremely helpful remarks of one of the anonymous referees concerning the use of Airy functions.

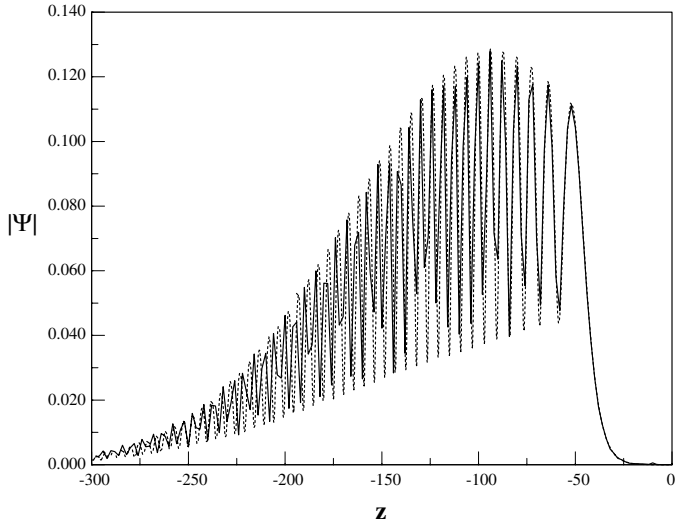

Figure 8. Numerical profile (dashed line) and analytical solution of equation (14) (solid line) for the thin packet of figure 1.

The wavefunction at all times then becomes

$$\Psi(x,t) = \int_{-\infty}^{\infty} C(a)\chi_a(x)\,\mathrm{e}^{-\mathrm{i}Et}\,\mathrm{d}a. \tag{14}$$

For thin enough wave packets $C(a)$ may be obtained analytically by extending the integration to $+\infty$ and neglecting corrections of order $\gamma = \frac{\sigma}{l_g}$, with σ the initial width of the packet. Under these approximations $C(a)$ becomes

$$C(a) = (2^3\pi\gamma^2)^{\frac{1}{4}} l_g \exp\left((a+x_0)\gamma^2 + \frac{2\gamma^6}{3}\right)\chi_a(a+x_0+\gamma^2) \tag{15}$$

where $x_0 = \frac{z_0}{l_g}$.

Inserting this formula into equation (14) we find the wavefunction at all times.

Figures 8 and 9 present the comparison of the numerical calculation for a thin packet and a wider packet to the analytical formula of equation (14) with the approximation of equation (15). The thin packet fit is quite good, while for the wider packet there is a discrepancy in the height of the peak. This discrepancy is due to the fact that γ for a wider packet is not negligible and the formula of equation (15) needs to be amended. However, in both cases the basic feature of the existence and absence of a diffractive train is evident. It is worth mentioning that there is no rescaling of either analytical or numerical data points.

The long-time behaviour of the thin packet as compared to a wide packet remains unchanged for as far as we could integrate the time-dependent Schrödinger equation numerically and still agrees with the analytical solution of equation (14). We reached a time of 30 ms and the profiles just spread, but do not change in shape. At that time the centre of the packet is around 4.5 mm below the mirror.

The integration of the equation becomes prohibitive beyond this time due to the strong oscillations in the wavefunction that require an increasingly smaller time step. The results, however, look quite firm. The diffractive structure persists for infinite times, as was found for the wave packet diffraction in space and time effect [1–5].

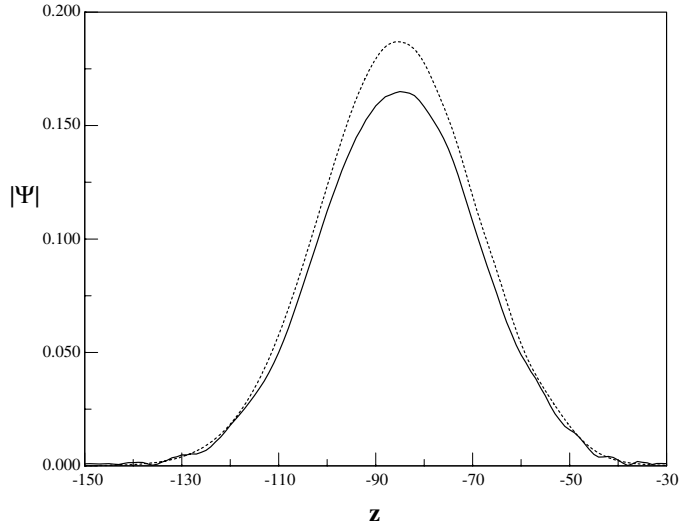

Figure 9. Numerical profile (dashed line) and analytical solution of equation (14) (solid line) for the wider packet of figure 1.

In the next section, we will provide some closing statements on the relevance of the falling packet effect for Bose–Einstein condensates and atom lasers.

4. Summary

We have found that a falling packet that is blocked by an obstacle *from above*, behaves differently depending on its initial spread. A packet wider than the gravitational mass-dependent length scale l_g falls almost as a free packet, whereas a thin packet has a distinctive diffraction pattern that propagates with it, analogous to the 'wave packet diffraction in space and time effect' [1–5].

We consider now a possible scenario to implement the findings of this work, and also take advantage of them for the purposes of creating an atom laser. Although there seems to be some controversy as to what an *atom laser* is [27], at a pedestrian level it would consist of a three stage machine: a feeding stage that pumps in atoms in an incoherent phase; a condensation cavity and a continuous output coupler. The investigation of these stages is as of today very advanced both theoretically and experimentally [28].

We would like to point out that the results of this paper suggest an alternative avenue for the continuous output coupling of a Bose–Einstein condensate.

Basically, it consists of an orifice, a physical one or one drilled in the mesh of laser radiation that confines the condensate. Through the orifice the condensate can exit in a pencil-like thin jet of atoms [12].

Position now a mirror above the atoms and let them fall freely while the feeding continues. It appears then that the outcome will be a coherent train of atoms having the characteristic oscillations found here, provided the width of the pencil is smaller than $\sqrt{l_g^3/|z_0|}$.

In order to see if this design works and check whether it fits the criteria of an atom laser set in [27], we need to perform at least a two-dimensional calculation with a source term. This endeavour is currently underway.

Acknowledgments

I would like to thank the anonymous referees for very valuable remarks.

References

[1] Kälbermann G 1999 *Phys. Rev.* A **60** 2573
[2] Kälbermann G 2001 *J. Phys. A: Math. Gen.* **34** 3841 (*Preprint* quant-ph 9912042)
[3] Kälbermann G 2001 *J. Phys. A: Math. Gen.* **34** 6465 (*Preprint* quant-ph 0008077)
[4] Kälbermann G 2002 Wavepacket diffraction in the Kronig–Penney model *J. Phys. A: Math. Gen.* **35** 1045 (*Preprint* cond-mat 0107522)
[5] Kälbermann G 2002 Single and double slit scattering of wave packets *J. Phys. A: Math. Gen.* **35** 4599
[6] Anderson M H, Ensher J R, Wiemann C E and Cornell E A 1995 *Science* **269** 198
[7] Davis K B, Mewes M-O, Andrews M R, Van-Druten N J, Durfee D S, Kurn D M and Ketterle W 1995 *Phys. Rev. Lett.* **75** 3969
[8] Mewes M-O, Andrews M R, Kurn D M, Durfee D S, Townsend C G and Ketterle W 1997 *Phys. Rev. Lett.* **78** 582
[9] Bloch I, Hänsch T W and Esslinger T 1999 *Phys. Rev. Lett.* **82** 3008
[10] Gerbier F, Bouyer P and Aspect A 2001 *Phys. Rev. Lett.* **86** 4729
[11] Nesvizhevsky V, Börner H, Petukhov A, Abele H, Baessler S, Ruess F, Stöferle T, Westphal A, Gagarski A, Petrov G and Strelkov A 2002 *Nature* **415** 297
[12] Bongs K, Burger S, Birkl G, Ertmer W, Rzazewki K, Sanpera A and Lewenstein M 1999 *Phys. Rev. Lett.* **83** 3577
[13] Peters A, Chung K Y and Chu S 1999 *Nature* **400** 849
[14] Moshinsky M 1952 *Phys. Rev.* **88** 625
[15] Brukner C and Zeilinger A 1997 *Phys. Rev.* A **56** 3804 and references therein
[16] Szriftgiser P, Guéry-Odelin D, Arndt M and Dalibard J 1997 *Phys. Rev. Lett.* **77** 4
[17] Gea-Banacloche J 1999 *Am. J. Phys.* **67** 776 and references therein
[18] Dodonov V V and Andreata M A 2000 *Phys. Lett.* A **275** 174
[19] Dalfovo F, Giorgini S, Pitaevskii L and Stringari S 1999 *Rev. Mod. Phys.* **71** 463
[20] Grisenti R E, Schöllkopf W, Toennies J P, Hegerfeldt C C and Köhler T 1999 *Phys. Rev. Lett.* **83** 1755
[21] Landau L D and Lifschitz E M 1965 *Quantum Mechanics* (London: Pergamon) p 79
[22] Greenberger D M 1980 *Am. J. Phys.* **48** 256
[23] Wadati M 1999 *J. Phys. Soc. Japan* **68** 2543
[24] Vandegrift G 2000 *Am. J. Phys.* **68** 576
[25] Vallée O 2000 *Am. J. Phys.* **68** 672
[26] Abramowitz M and Stegun I A (ed) 1972 *Handbook of Mathematical Functions* (New York: Dover) section 10.4
[27] Wiseman H M 1997 *Phys. Rev.* A **56** 2068
Wiseman H M 1998 *Phys. Rev.* **57** 674
[28] Ballagh R J and Savage C M 2000 *Mod. Phys. Lett.* B **14** (Suppl S) 153 (*Preprint* cond-mat/0008070)